Theoretical Study of Addition Reactions of Heavy Carbenes to Carbon and Boron Nitride Nanotubes

Ming-Der Su*

Department of Applied Chemistry, National Chiayi University, Chiayi 60004, Taiwan, Republic of China

Received: June 25, 2005; In Final Form: September 17, 2005

In an effort to gain insight into the activation energies and reaction enthalpies of the chemical functionalization of carbon and boron nitride nanotubes, calculations using density functional theory have been carried out for the cycloaddition of a heavy carbene to a single-walled carbon (SWCNT; $C_{130}H_{20}$) and a boron nitride (SWBNNT; $B_{65}N_{65}H_{20}$) nanotube. The $(CH_3)_2X$ + SWCNT and $(CH_3)_2X$ + SWBNNT (X = C, Si, Ge, Sn, and Pb) reactions are the subject of the present study. All the stationary points were determined at the B3LYP/LANL2DZ level of theory. The major conclusions that can be drawn from this work are as follows: (i) Considering both the activation barrier and reaction enthalpy based on the model calculations presented here, it is found that the order of $(CH_3)_2X$ reactivity is X = C > Si ≫ Ge > Sn > Pb, irrespective of whether cycloaddition is to a SWCNT or a SWBNNT sidewall. That is to say, $(CH_3)_2C$ and $(CH_3)_2Si$ can readily add to the sidewalls of SWCNT and SWBNNT, whereas $(CH_3)_2Ge$, $(CH_3)_2Sn$, and $(CH_3)_2Pb$ are unreactive. (ii) Since the chemical reactivities of SWCNT and SWBNNT sidewalls closely resemble those of the small $C_{16}H_{10}$ and $B_8N_8H_{10}$ molecules, at least in a qualitative sense, the use of the above small molecules as models is sufficient to provide qualitatively correct results. (iii) Our theoretical observations indicate that all the (5,5) SWCNT and SWBNNT cycloadducts favor opened rather than closed three-membered ring structures. (iv) The theoretical investigations demonstrate that the singlet−triplet splitting of the carbene species (R_2X) as well as that of the small model molecules can be used as a diagnostic tool to predict the addition reactivities of carbene analogues and sidewalls of various nanotubes, respectively. Moreover, the results obtained in this work allow a number of predictions to be made.

I. Introduction

Carbon nanotubes,[1] in particular single-walled carbon nanotubes (SWCNTs), are a material that has been extensively studied both experimentally and theoretically during the past decade.[2] Their popularity is due, in large part, to their having remarkable mechanical and electronic properties that make them likely candidates for components in molecular-scale machines and electronics. To be able to expand application of carbon nanotubes into new areas, it will be necessary to functionalize them controlled ways that ensure good mechanical and electrical contact between the tubes and the other components of the devices. Besides this, some problems in reactions with carbon nanotubes are their low solubility or dispersability, and their occurrence in bundles. It is therefore a general belief that chemical derivatization of nanotubes is desirable to improve their solubility and processibility[3,4] and to lead to a significant enhancement in the properties relevant to their practical applications.[5] As a result, not surprisingly, the field of carbon nanotube functionalization is growing rapidly.[3,6,7]

Equally interesting are non-carbon nanotubes.[8] Compounds with a propensity for graphite-like layering are natural candidates for nanotube formation, and indeed hexagonal boron nitride (BN) based nanotubes have been variously predicted[9] and observed.[10] In principle, a BN nanotube is the inorganic analogue of a carbon nanotube, obtained by replacing each carbon with alternating boron and nitrogen atoms in a honeycomb network. The BN nanotubes have been found to be much more stable with respect to oxidation in air and have excellent thermal and chemical stability.[11] This strongly suggests that BN nanotubes may provide interesting possibilities for potential device applications,[12] just as in the case of the carbon nanotubes. Despite this obvious potential, no successful methods have been reported for functionalizing BN nanotubes.[13] In fact, previous studies have largely demonstrated the synthesis and stoichiometric characterization of multiwalled BN nanotubes.[10,14] To the best of our knowledge, neither experimental nor theoretical studies have been devoted to the study of the chemical reactivity of BN nanotubes.

Recently, through the elegant studies performed by Hirsch and co-workers,[7] it was found that the direct fuctionalization of SWCNTs with organic groups is possible using reactive species such as carbenes, nitrenes, and radicals. For instance, they reported that especially stable solutions of functionalized SWCNTs are formed from the addition of nucleophilic carbenes.[7a] It is these fascinating experimental results that inspire this study. Obviously, these novel experiments left several questions unsolved, including the following: (a) If carbenes can be used as reagents for chemical additions to the sidewalls of carbon nanotubes, would it be possible to extend this to other heavier carbenes or carbene analogues? (b) What are the relative reactivities for the addition of carbenes to various nanotubes? (c) What are the structures and energetics of the assumed intermediates and transition states (TSs) involved in such cycloaddition reactions? (d) What factors control the absolute magnitudes of the activation barriers and the enthalpies for such nanotube addition reactions? As mentioned earlier, no estimates

* E-mail: midesu@mail.ncyu.edu.tw.

10.1021/jp053452c CCC: $30.25
Published on Web 10/20/2005

of geometries and energetics are available yet from experiments. The reason for this is mainly because, despite impressive progress in this field, there is still great difficulty in obtaining reasonable quantities of highly purified nanotubes,[6c] let alone being able to obtain the precise physical parameters of the nanotubes required for analysis and interpretation. Additionally, it is very difficult to detect the intermediate as well as the TS due to limitations in current experimental techniques. Theory is therefore a potentially useful partner to experiment in the investigation of the mechanism of these reactions. In view of the situation, theoretical information should be of great help for further advance in nanotube chemistry.[15]

To shed some light on the above open questions, we have computed the energy profiles for the cycloaddition reactions of armchair nanotubes with model compounds $(CH_3)_2X$ (X = C, Si, Ge, Sn, and Pb), shown in eqs 1 and 2, using the density functional theory (DFT).[16,17]

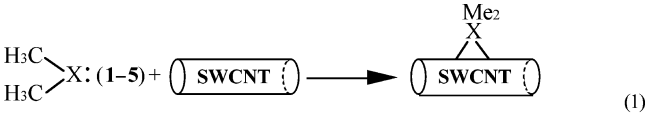

(1)

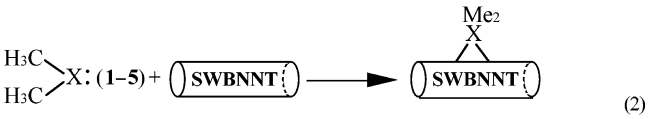

(2)

That is, five methyl-substitubted carbene analogues, methylene ($(CH_3)_2C$) **1**, silylene ($(CH_3)_2Si$) **2**, germylene ($(CH_3)_2Ge$) **3**, stannylene ($(CH_3)_2Sn$) **4**, and plumbylene ($(CH_3)_2Pb$) **5**, were selected as model reactants for investigation of their reaction mechanisms. In eqs 1 and 2, each reacts with an armchair SWCNT or an armchair single-walled BN nanotube (SWBNNT) in a three-membered ring formation reaction. For comparison, we have also studied the addition of $(CH_3)_2X$ (**1**−**5**) to the isoelectronic $C_{16}H_{10}$ (**6**) and $B_8N_8H_{10}$ (**7**) species, as shown in eqs 3 and 4, respectively.

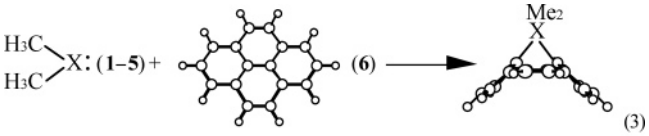

(3)

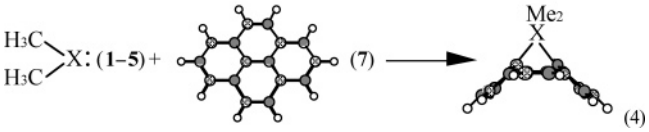

(4)

Choosing eqs 1 and 2 as model systems for studying the cycloaddition reactions of nanotubes with carbene species is of interest for several reasons. First, it is well accepted that single-walled nanotubes are of scientific importance because the study of their intrinsic physical properties is possible and easy.[18] Hence, to reduce the complexity of the problem, we chose the single-walled nanotubes (i.e., SWCNT and SWBNNT) as model reactants in which the determining variable is the efficiency of cycloaddition reactions. Second, it should be pointed out that our focus on the methyl-substituted carbene species does not imply that other substitution effects within the carbene itself are not important. It means only that we acknowledge the complexity of the problem and choose to treat the $(CH_3)_2X$: species aspects separately. Carbene substitution can be considered later, and it may or may not affect the three-membered ring formation reactions. Third, the previous study of armchair, zigzag, and chiral single-walled carbon nanotubes found that the most thermodynamically stable configuration is the armchair single-walled carbon nanotube.[19] Thus, in this work we have undertaken a theoretical investigation into the cycloaddition of carbene and carbene analogues to armchair SWCNTs and SWBNNTs. Fourth, initial speculation suggested that chemical functionalization of single-walled nanotubes would be most favorable at their end caps and that functionalization of single-walled nanotube sidewalls would be difficult to achieve.[20] Nevertheless, successful controlled functionalization of single-walled carbon nanotube sidewalls leading to soluble products has recently been reported.[7,21] This may provide a vital precursor for the subsequent attachment of a wide variety of functional groups to the exterior of the single-walled nanotubes. It is therefore hoped that our theoretical study will provide a crucial starting point for developing a detailed understanding of single-walled nanotube sidewall chemistry. Fifth, according to previous theoretical studies, a variety of quantum chemical methods have been tried, such as semiempirical[22] and Hartree−Fock[23] calculations. Nevertheless, on one hand, although semiempirical methods have been proved to be an accessible and useful tool to describe some properties of carbon nanotubes, they are notorious for their unreliable estimates of geometries as well as energies. On the other hand, due to the large size of nanotubes, carefully chosen truncated models, appropriate for the problem being investigated, are required. One available approach is to use the ONIOM technique,[24] which combines a low- and high-level theory to allow a more realistic treatment of the system. This strategy presumably allows larger systems to be simulated at a practical computational cost.[25] Nevertheless, it was recently reported that the often-used ONIOM(B3LYP:AM1) approach is not appropriate for the nanotube systems studied, since serious limitations in the ONIOM approach to computational nanotube chemistry are apparent.[26,27] Accordingly, to obtain the more precise chemical information, the DFT method was applied in this study to investigate the reaction mechanism as well as chemical reactivity in single-walled nanotubes.

Through this theoretical study, we hope (a) to obtain a detailed understanding of the sidewall reactivity of C and BN nanotubes, (b) to investigate the influence of the central atom of $(CH_3)_2X$ upon the geometries and energies of the transition states and products, (c) to elucidate the differences between SWCNTs and SWBNNTs, and (d) to investigate those factors controlling the activation barrier for the three-membered ring formation reactions. Finally, our aim is to search for a general theory of reactivity for such cycloaddition reactions and to decide whether the reactivity can be predicted through a qualitative understanding of the reaction mechanisms of simpler systems using either simple molecular orbital or valence bond arguments.[30] It will be shown that an understanding of the factors that can facilitate chemical functionalization of both SWCNTs and SWBNNTs may suggest further synthetic applications.

II. Computational Details

All geometries were fully optimized without imposing any symmetry constraints, although in some instances the resulting structure showed various elements of symmetry. DFT was employed with the three-parameter hybrid exchange functional of Becke[16] and the Lee, Yang, and Parr correlation functional.[17] This functional is commonly known as B3LYP, which was carried out with relativistic effective core potentials on group 14 elements modeled using the double-ζ (DZ) basis sets.[30] Thus, the model compounds $(H_3C)_2X$·SWCNT and $(H_3C)_2X$·SWBNNT have 1248 (822 electrons) basis functions for X = C, Si, Ge,

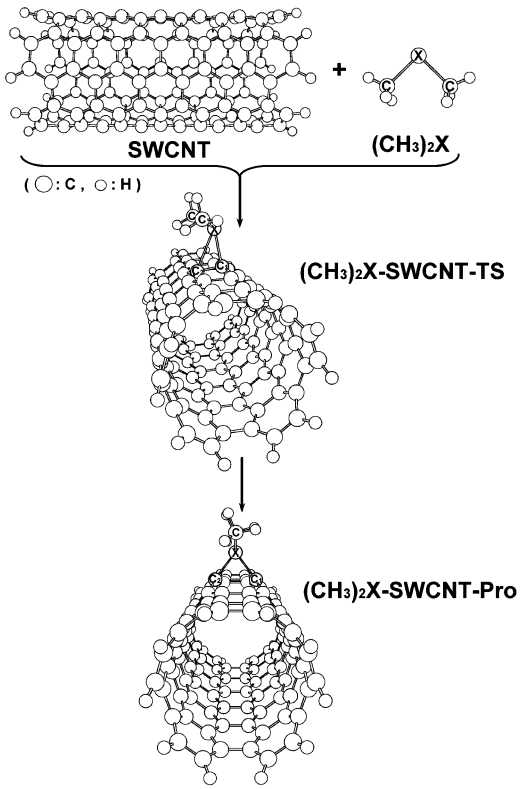

Figure 1. Reference geometry for the model reaction: $(CH_3)_2X$ + SWCNT. For the selected bond lengths and bond angles as well as relative energies, see Tables 1 and 3.

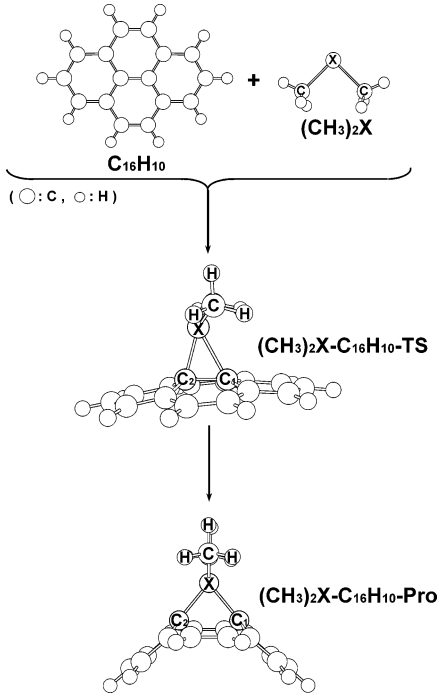

Figure 2. Reference geometry for the model reaction: $(CH_3)_2X$ + $C_{16}H_{10}$. For the selected bond lengths and bond angles as well as relative energies, see Tables 2 and 3.

TABLE 1: Selected Optimized Geometrical Parameters for the Stationary Points Depicted in Figure 1[a]

	X = C	X = Si	X = Ge	X = Sn	X = Pb
			Me_2X		
X−C	1.505	1.931	2.029	2.197	2.267
∠C−X−C	112.7	97.82	95.62	93.58	93.02
			TS		
X−C	1.512	1.914	1.974	2.127	2.193
∠C−X−C	113.3	105.6	113.5	121.7	131.4
X−C_1	2.284	2.225	2.063	2.173	2.276
X−C_2	2.783	2.629	2.340	2.192	2.278
C1−C_2	1.459	1.507	1.572	1.743	1.662
∠X−C_1−C_2	93.45	87.36	78.84	65.90	68.60
			Pro		
X−C	1.562	1.892	1.961	2.124	2.196
∠C−X−C	101.3	106.0	108.7	110.5	107.5
X−C_1	1.545	1.891	1.958	2.117	2.191
X−C_2					
C_1−C_2	2.161	2.377	2.404	2.459	2.488
∠X−C_1−C_2	45.63	51.07	52.15	54.49	56.98

[a] All data were obtained by the B3LYP/LANL2DZ approach. The energy is given with respect to the reactants in the respective reaction. That is, Me_2X + SWCNT → transition state (TS) → product (Pro). The angles are given in deg, distances in Å. The corresponding geometrical arrangement is depicted for a simpler overview. See Figure 1. The C_1−C_2 bond length in a bare SWCNT is calculated to average 1.436 Å at the B3LYP/LANL2DZ level of theory.

Sn, and Pb. Moreover, the restricted B3LYP approach was used in this work to describe all the stationary points, except for the triplet states of reactants, which were described by unrestricted wave functions. Hence, all the B3LYP calculations are denoted by B3LYP/LANL2DZ. Vibrational frequency calculations at the RHF/LANL2DZ level were used to characterize all stationary points as either minima (no imaginary frequencies) or transition states (one imaginary frequency). Then these stationary points were further calculated at the B3LYP/LANL2DZ level using the opt=readfc keyword. Due to the limitation of both CPU time and memory size available, the B3LYP zero-point energy (ZPE) could not be applied for all of the SWCNT and SWBNNT systems in the present work. That is, because frequencies were not calculated for all species at the B3LYP/LANL2DZ level of theory, ZPE corrections were not performed. Nevertheless, the addition of these corrections would not change our conclusions. All the calculations were performed with the GAUSSIAN 03 package of programs.[31]

The simulation models used in this study consist of the (5,5) armchair SWCNT and SWBNNT,[32] as shown at the top of Figures 1 and 4, respectively. The dangling bonds at both ends are terminated with H atoms, yielding the $C_{130}H_{20}$ and $B_{65}N_{65}H_{20}$ tubes. Both optimal diameters at the B3LYP/LANL2DZ level are about 7.07 and 7.22 Å, respectively.

III. Results and Discussion

(1) The SWCNT System. The results of this work are given in Figures 1 and 2, which contain the reaction profiles computed for the model systems in eqs 1 and 3.[33] Basically, the results for three regions on the potential energy surfaces will be presented: $(H_3C)_2X$ (X = C, Si, Ge, Sn, and Pb) + SWCNT or $C_{16}H_{10}$ (**6**), the TS, and the cycloaddition product (Pro). Some selected geometrical parameters optimized for the stationary points can be taken from Tables 1 and 2. The corresponding relative energies at the B3LYP/LANL2DZ level of theory are collected in Table 3. The potential energy profiles at the B3LYP level are therefore summarized in Figure 3. Cartesian coordinates for these stationary points are included in the Supporting Information. Several important conclusions can be drawn from these figures and tables.

First, we have located the transition state for each $(H_3C)_2X$ species (Me_2C-SWCNT-TS, Me_2Si-SWCNT-TS, Me_2Ge-SWCNT-TS, Me_2Sn-SWCNT-TS, and Me_2Pb-SWCNT-TS) at both RHF and B3LYP levels of theory. Our RHF/LANL2DZ

TABLE 2: Selected Optimized Geometrical Parameters for the Stationary Points Depicted in Figure 2[a]

	X = C	X = Si	X = Ge	X = Sn	X = Pb
			Me_2X		
X−C	1.505	1.931	2.029	2.197	2.267
∠C−X−C	112.7	97.82	95.62	93.58	93.02
			TS		
X−C	1.513	1.896	1.959	2.130	2.182
∠C−X−C	113.6	115.7	121.7	128.1	138.6
$X-C_1$	2.035	1.987	2.002	2.213	2.324
$X-C_2$	2.598	2.200	2.062	2.223	2.325
C_1-C_2	1.472	1.543	1.608	1.586	1.559
$\angle X-C_1-C_2$	94.27	75.92	68.69	68.72	70.46
			Pro		
X−C	1.556	1.892	1.966	2.132	2.164
∠C−X−C	102.2	107.6	109.9	110.4	114.1
$X-C_1$	1.528	1.878	1.950	2.113	2.138
$X-C_2$					
C_1-C_2	2.165	2.420	2.462	2.497	2.410
$\angle X-C_1-C_2$	44.91	49.90	50.86	53.78	55.70

[a] All data were obtained by the B3LYP/LANL2DZ approach. The energy is given with respect to the reactants in the respective reaction. That is, $Me_2X + C_{16}H_{10}$ → transition state (TS) → product (Pro). The angles are given in deg, distances in Å. The corresponding geometrical arrangement is depicted for a simpler overview. See Figure 2. The C═C bond length in a bare $C_{16}H_{10}$ is calculated to be 1.435 Å at the B3LYP level of theory.

TABLE 3: Relative Energies for Singlet and Triplet Me_2X (X = C, Si, Ge, Sn, and Pb) and for the Process: Reactans → Transition State → Cycloaddition Product[a]

system	ΔE_{st}[b] (kcal mol^{-1})	$\Delta E^{\ddagger}$ (kcal mol^{-1})	ΔH (kcal mol^{-1})
$(CH_3)_2C$ + SWCNT	+1.95	+3.19	−60.1
$(CH_3)_2Si$ + SWCNT	+21.6	+6.08	−18.5
$(CH_3)_2Ge$ + SWCNT	+27.6	+13.5	+0.575
$(CH_3)_2Sn$ + SWCNT	+29.4	+24.2	+21.1
$(CH_3)_2Pb$ + SWCNT	+37.0	+49.4	+50.1
$(CH_3)_2C + C_{16}H_{10}$	+1.95	+16.0	−20.2
$(CH_3)_2Si + C_{16}H_{10}$	+21.6	+32.5	+25.8
$(CH_3)_2Ge + C_{16}H_{10}$	+27.6	+46.1	+45.7
$(CH_3)_2Sn + C_{16}H_{10}$	+29.4	+62.1	+68.9
$(CH_3)_2Pb + C_{16}H_{10}$	+37.0	+84.0	+100

[a] All data were obtained by the B3LYP/LANL2DZ approach for eqs 1 and 3, respectively. The energy is given with respect to the reactants in the respective reaction. Potential energy surfaces for the addition of Me_2X to the SWCNT are summarized in Figure 3. [b] Singlet and triplet energy splitting for the Me_2X species. A positive value means the singlet is the ground state.

frequency calculations suggest that the main component of the transition vector corresponds to the displacement of the $(H_3C)_2X$ toward the C═C fragment of the SWCNT, whose eigenvalue gives an imaginary frequency of 496i (Me_2C-SWCNT-TS), 398i (Me_2Si-SWCNT-TS), 302i (Me_2Ge-SWCNT-TS), 222i (Me_2Sn-SWCNT-TS), and 145i (Me_2Pb-SWCNT-TS). Additionally, the B3LYP calculations also indicate that the transition states for the SWCNT cycloaddition reaction become less asynchronous as the central atom X changes from C down to Pb. That is, the forming $X-C_1$ bond becomes far more advanced than the forming $X-C_2$ bond. As can be seen in Table 1, in each case one of the forming bonds ($X-C_1$) is longer than a normal X−C single bond of a cycloaddition product (i.e., Me_2C-SWCNT-TS, 2.28 Å; Me_2Si-SWCNT-TS, 2.23 Å; Me_2Ge-SWCNT-TS, 2.06 Å; Me_2Sn-SWCNT-TS, 2.17 Å; and Me_2Pb-SWCNT-TS, 2.28 Å), while the other ($X-C_2$) is considerably stretched (i.e., Me_2C-SWCNT-TS, 2.78 Å; Me_2Si-SWCNT-TS, 2.63 Å; Me_2Ge-SWCNT-TS, 2.34 Å; Me_2Sn-SWCNT-TS, 2.19 Å; and Me_2Pb-SWCNT-TS, 2.28 Å). This finding can be explained in terms of the atomic size of the group 14 element X. In principle, it is believed that if the central atom X has a small atomic radius, this leads to a large steric effect between the $(H_3C)_2X$ fragment and the SWCNT, increasing asynchronicity in bond formation. Despite the dramatic asynchronicity in these transition structures, the present calculations indicate that the SWCNT cycloaddition reaction is still concerted, since no energy minimum corresponding to an intermediate between the transition state and products has been found.

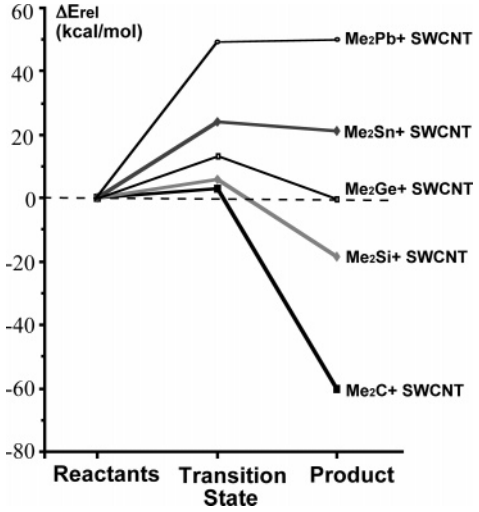

Figure 3. Potential energy surfaces for the cycloadditions of various $(CH_3)_2X$ to SWCNT. The relative energies are taken from the B3LYP/LANL2DZ level as given in Table 3. For the B3LYP optimized structures of the stationary points, see Table 1 and Supporting Information.

Second, the expected products of the addition reactions of $(H_3C)_2X$ with SWCNT are the three-membered ring cycloadducts. However, in contrast to earlier theoretical studies[24b] and experimental expectation, our full B3LYP/LANL2DZ computations on nanotube models studied in this work reveal that SWCNT with $(H_3C)_2X$ addends favor opened rather than closed three-membered ring structures. For instance, as one can see in Table 1, the C_1-C_2 bond length in the cycloadduct is calculated to be 2.16 Å (Me_2C-SWCNT-Pro), 2.38 Å (Me_2Si-SWCNT-Pro), 2.40 Å (Me_2Ge-SWCNT-Pro), 2.46 Å (Me_2Sn-SWCNT-Pro), and 2.49 Å (Me_2Pb-SWCNT-Pro), which are all much larger than that of pristine SWCNT (1.44 Å). This conclusion also holds true for the smaller model system of $(H_3C)_2X$ (**1**−**5**) + $C_{16}H_{10}$ (**6**). As shown in Table 2, the C_1-C_2 bond length in the cycloproduct is predicted to be 2.17 Å (Me_2C-$C_{16}H_{10}$-Pro), 2.42 Å (Me_2Si-$C_{16}H_{10}$-Pro), 2.46 Å (Me_2Ge-$C_{16}H_{10}$-Pro), 2.50 Å (Me_2Sn-$C_{16}H_{10}$-Pro), and 2.41 Å (Me_2Pb-$C_{16}H_{10}$-Pro), much larger than that calculated for prime $C_{16}H_{10}$ (1.44 Å). Indeed, our theoretical results are in excellent agreement with one recent theoretical report.[26,27] Namely, the sidewall of SWCNTs should be opened by chemical modifications.[28,29,34]

Third, it is evident, from both a kinetic and thermodynamic viewpoint, that the SWCNT cycloaddition reaction of a carbene analogue bearing a more electronegative central atom is much more favorable than that bearing a less electronegative central atom. For instance, as seen in Table 3, the activation barriers from the reactants to the transition state at the present level of theory increase in the order Me_2C-SWCNT-TS (3.2 kcal/mol) < Me_2Si-SWCNT-TS (6.1 kcal/mol) < Me_2Ge-SWCNT-TS (14 kcal/mol) < Me_2Sn-SWCNT-TS (24 kcal/mol) < Me_2Pb-SWCNT-TS (49 kcal/mol). Likewise, the reaction enthalpies increase in the order Me_2C-SWCNT-Pro (−60 kcal/mol) < Me_2Si-SWCNT-Pro (−18 kcal/mol) < Me_2Ge-SWCNT-Pro

(0.58 kcal/mol) < Me_2Sn-SWCNT-Pro (21 kcal/mol) < Me_2Pb-SWCNT-Pro (50 kcal/mol). That is to say, for SWCNT cycloadditions there is a very clear trend toward higher activation barriers and more endothermic (or less exothermic) reactions on going from C to Pb. It should be noted that the energies of the products Me_2Ge-SWCNT-Pro, Me_2Sn-SWCNT-Pro, and Me_2Pb-SWCNT-Pro are above those of their corresponding starting materials. This strongly implies that the cycloadditions of germylene, stannylene, and plumbylene to a SWCNT are energetically unfavorable and would be endothermic. Namely, our computational results indicate that the functionalization products of nanotubes with heavy carbenes Me_2X are not produced directly from the cycloaddition reactions of eq 1 but possibly exist if these final products are produced through other reaction pathways.

Fourth, on the other hand, the same phenomena can also be found in the $(H_3C)_2X + C_{16}H_{10}$ (**6**) addition reactions (i.e., eq 3).[33] As seen in Table 3, it is apparent that the B3LYP barrier height (relative to the corresponding reactants) for the cycloaddition reaction increases in the order Me_2C-$C_{16}H_{10}$-TS (16 kcal/mol) < Me_2Si-$C_{16}H_{10}$-TS (33 kcal/mol) < Me_2Ge-$C_{16}H_{10}$-TS (46 kcal/mol) < Me_2Sn-$C_{16}H_{10}$-TS (62 kcal/mol) < Me_2Pb-$C_{16}H_{10}$-TS (84 kcal/mol). Moreover, the reaction enthalpy for these carbene analogues follows the similar trend to the activation energy: Me_2C-$C_{16}H_{10}$-Pro (−20 kcal/mol) < Me_2Si-$C_{16}H_{10}$-Pro (+26 kcal/mol) < Me_2Ge-$C_{16}H_{10}$-Pro (+46 kcal/mol) < Me_2Sn-$C_{16}H_{10}$-Pro (+69 kcal/mol) < Me_2Pb-$C_{16}H_{10}$-Pro (+100 kcal/mol). Consequently, we predict that the reactivity of $(H_3C)_2X$ species toward $C_{16}H_{10}$ decreases with increasing atomic weight of the central atom X. This conclusion is consistent with some available experimental as well as theoretical findings.[35]

Fifth, from the above data analysis, it is found that the trend for carbenic reactivity toward the sidewall of a carbon nanotube is the same as that toward the C═C double bond of a $C_{16}H_{10}$ (**6**) molecule. For example, our model calculations show that, irrespective of whether addition is to a bulky (e.g., SWCNT) or small (e.g., $C_{16}H_{10}$) unsaturated carbon containing system, addition of a carbene analogue containing a lighter or a more electronegative central atom will be favored from both a thermodynamic and a kinetic point of view. Nevertheless, our computational results also indicate that the barrier height for the cycloaddition of $(H_3C)_2X$ to a SWCNT is lower than that to $C_{16}H_{10}$ (**6**) for a given central atom X. Likewise, the reaction enthalpy for cycloaddition to SWCNT sidewalls is more endothermic than to $C_{16}H_{10}$ for the same center element X. This may be due to the fact that repulsions between the $(H_3C)_2X$ species and the sidewall of a SWCNT are smaller than those between the $(H_3C)_2X$ molecule and a $C_{16}H_{10}$ *planar* molecule.

In short, the present calculations suggest the following about the cycloaddition mechanism for the $(H_3C)_2X$ (**1**−**5**) + SWCNT reactions: (a) Considering both the calculated activation barriers and reaction enthalpies, we conclude that the $(H_3C)_2X$ order of reactivity is X = C > Si ≫ Ge > Sn > Pb. This trend is in accordance with that found in the smaller model system of $(H_3C)_2X$ (**1**−**5**) + $C_{16}H_{10}$ (**6**). (b) The three-membered ring formation reaction is not only concerted (proceeding without formation of an intermediate) but also asynchronous (with the X−C bond forming not occurring simultaneously in the transition states). (c) Our theoretical findings strongly suggest that all the (5,5) SWCNT adducts favor opened structures rather than three-membered rings. (d) The cycloadditions become ever more endothermic (or less exothermic) down the column of group 14 elements, reflecting the weaker X−C bond as X changes from C down to Pb. (e) Since the chemical reactivity of SWCNT sidewall resembles that of the small $C_{16}H_{10}$ molecule, the use of the latter molecule as a model is sufficient to provide qualitatively correct results. (f) Note that the energetics of the (5,5) armchair SWCNT derivatives investigated here are above those of their corresponding transition states. Our theoretical findings thus suggest that the cycloaddition products might possibly exist if these compounds (i.e., $(H_3C)_2X$·SWCNT) are produced through other reaction paths, rather than the eq 1 pathway.

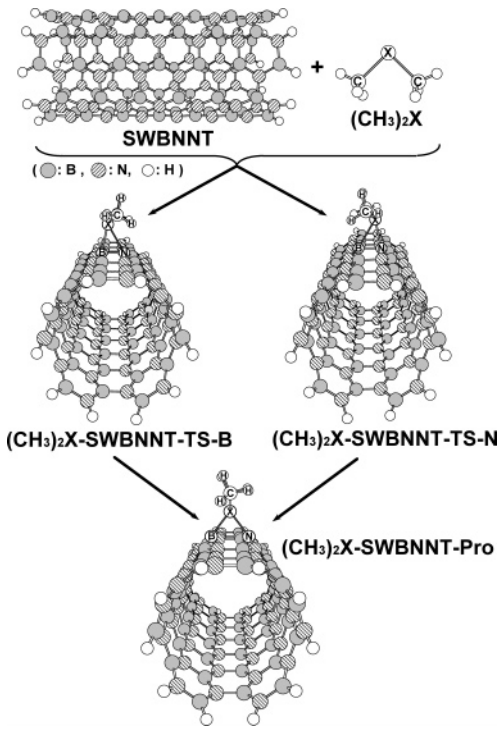

Figure 4. Reference geometry for the model reaction $(CH_3)_2X$ + SWBNNT. See the text. For selected bond lengths and bond angles as well as relative energies, see Tables 4 and 6.

(2) The SWBNNT System. The results for this section are given in Figures 4 and 5, which include the reaction profiles computed for the model systems eqs 2 and 4. Again, the results for three regions on the potential energy surfaces will be presented: $(H_3C)_2X$ (X = C, Si, Ge, Sn, and Pb) + SWBNNT or $B_8N_8H_{10}$ (**7**), the transition states (TS−B and TS−N), and the cycloaddition product (Pro). Some selected geometrical parameters optimized for those stationary points can be found in Tables 4 and 5, respectively. The corresponding relative energies at the B3LYP/LANL2DZ level of theory are collected in Table 6. The potential energy profiles for the $(H_3C)_2X$ + SWBNNT reactions at the B3LYP level are therefore summarized in Figure 6. Cartesian coordinates calculated for the stationary points at the B3LYP level are available as Supporting Information. Several major conclusions that can be obtained from the current study are given as follows.

First, the results for the cycloaddition of a $(H_3C)_2X$ to a SWBNNT are the most interesting aspect of the present study, since nothing was previously known about the barrier heights as well as enthalpies. In the case of the B═N doubly bonded systems, one can consider two paths of $(H_3C)_2X$ approach depicted in **8**. In path A, the $(H_3C)_2X$ attacks the boron atom of the B═N bond (B attack, see **8a**), whereas in path B, it attacks the nitrogen atom (N attack, see **8b**). In both paths, the $(H_3C)_2X$ plane is assumed to be parallel with the B═N bond (nonleast motion); any structure with the $(H_3C)_2X$ plane perpendicular

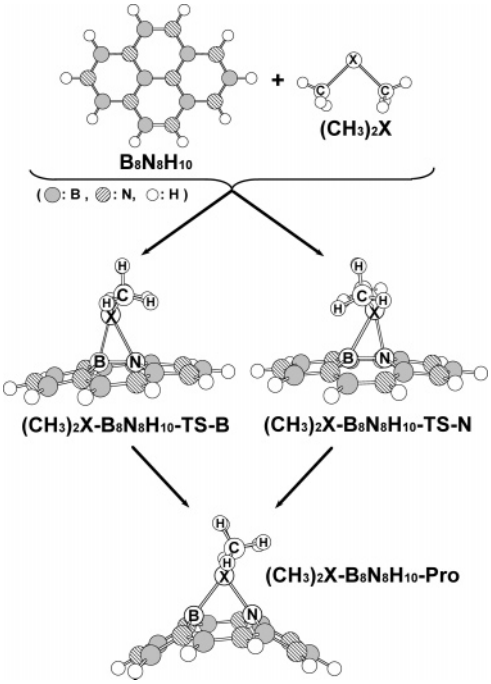

Figure 5. Reference geometry for the model reaction $(CH_3)_2X + B_8N_8H_{10}$. For selected bond lengths and bond angles as well as relative energies, see Tables 5 and 6.

TABLE 4: Selected Optimized Geometrical Parameters for the Stationary Points Depicted in Figure 4[a]

	X = C	X = Si	X = Ge	X = Sn	X = Pb
			Me_2X		
X−C	1.505	1.931	2.029	2.197	2.267
∠C−X−C	112.7	97.82	95.62	93.58	93.02
			TS-B		
X−C	1.513	1.918	2.004	2.125	2.204
∠C−X−C	111.9	98.32	98.34	98.13	97.90
X−B	2.968	2.406	2.495	2.571	2.610
X−N	2.865	2.512	2.617	2.628	2.770
B−N	1.467	1.515	1.519	1.542	1.529
∠X−B−N	71.59	75.94	77.18	76.78	79.36
			TS-N		
X−C	1.523	1.910	1.982	2.150	2.198
∠C−X−C	118.3	121.2	124.9	131.3	141.2
X−B	2.414	2.289	2.297	2.432	2.491
X−N	1.742	2.011	2.093	2.273	2.394
B−N	1.520	1.601	1.619	1.634	1.613
∠X−N−B	95.28	77.71	75.23	75.01	74.03
			Pro		
X−C	1.555	1.894	1.968	2.139	2.198
∠C−X−C	103.2	106.2	106.7	107.6	107.2
X−B	1.596	1.993	2.055	2.231	2.266
X−N	5.163	1.852	1.942	2.110	2.218
B−N	2.239	2.489	2.512	2.534	2.553
∠X−B−N	44.30	47.22	49.08	52.09	55.90

[a] All data were obtained by the B3LYP/LANL2DZ approach. The energy is given with respect to the reactants in the respective reaction. That is, Me_2X + SWBNNT → transition state (TS) → product (Pro). The angles are given in deg, distances in Å. See Figure 4. The B-N bond length in a bare SWBNNT is calculated to average 1.455 Å at the B3LYP/LANL2DZ level of theory.

to the B═N bond (least motion) is unstable due to the orbital symmetry rule.[36] All the transition states at the RHF/LANL2DZ level of theory were confirmed by calculation of the energy Hessian which shows only one imaginary frequency. That is, for the B attack path, 173i (Me_2C-SWBNNT-B-TS), 182i (Me_2Si-SWBNNT-B-TS), 185i (Me_2Ge-SWBNNT-B-TS), 106i (Me_2Sn-SWBNNT-B-TS), and 131i (Me_2Pb-SWBNNT-B-TS), while for the N attack path, 679i (Me_2C-SWBNNT-N-TS), 678i (Me_2Si-SWBNNT-N-TS), 472i (Me_2Ge-SWBNNT-N-TS), 359i (Me_2Sn-SWBNNT-N-TS), and 385i (Me_2Pb-SWBNNT-N-TS). It should be mentioned that the primary similarity between all

TABLE 5: Selected Optimized Geometrical Parameters for the Stationary Points Depicted in Figure 5[a]

	X = C	X = Si	X = Ge	X = Sn	X = Pb
			Me_2X		
X−C	1.505	1.931	2.029	2.197	2.267
∠C−X−C	112.7	97.82	95.62	93.58	93.02
			TS-B		
X−C	1.500	1.914	1.997	2.044	2.121
∠C−X−C	113.8	104.5	106.1	111.9	103.6
X−B	2.584	2.251	2.363	2.418	2.560
X−N	2.956	2.379	2.589	2.723	2.983
B−N	1.472	1.534	1.523	1.536	1.505
∠X−B−N	89.17	75.21	80.39	87.45	90.60
			TS-N		
X−C	1.518	1.910	1.977	2.145	2.192
∠C−X−C	119.2	121.2	130.1	136.0	149.7
X−B	2.254	2.289	2.291	2.448	2.540
X−N	1.687	2.011	2.109	2.301	2.468
B−N	1.498	1.601	1.559	1.560	1.544
∠X−N−B	89.89	77.71	75.63	76.02	74.61
			Pro		
X−C	1.547	1.893	1.969	2.140	2.201
∠C−X−C	104.7	106.9	107.3	106.9	105.6
X−B	1.576	1.976	2.037	2.215	2.253
X−N	1.545	1.842	1.949	2.107	2.191
B−N	2.203	2.438	2.385	2.460	2.516
∠X−B−N	44.54	47.94	51.58	53.25	54.36

[a] All data were obtained by the B3LYP/LANL2DZ approach. The energy is given with respect to the reactants in the respective reaction. That is $Me_2X + B_8N_8H_{10}$ → transition state (TS) → product (Pro). The angles are given in deg, distances in Å. See Figure 5. The B═N bond length in a bare $B_8N_8H_{10}$ is calculated to be 1.458 Å at the B3LYP/LANL2DZ level of theory.

TABLE 6: Relative Energies for Singlet and Triplet Me_2X (X = C, Si, Ge, Sn, and Pb) and for the Process: Reactans → Transition State → Cycloaddition Product[a]

system	ΔE_{st}[b] (kcal mol^{-1})	$\Delta E^{\ddagger}$[c] (kcal mol^{-1})	ΔH (kcal mol^{-1})
$(CH_3)_2C$ + SWBNNT	+1.95	−3.41 (B) +19.4 (N)	−61.7
$(CH_3)_2Si$ + SWBNNT	+21.6	+4.01 (B) +33.5 (N)	−18.6
$(CH_3)_2Ge$ + SWBNNT	+27.6	+11.5 (B) +44.7 (N)	−1.85
$(CH_3)_2Sn$ + SWBNNT	+29.4	+15.9 (B) +52.8 (N)	+15.1
$(CH_3)_2Pb$ + SWBNNT	+37.0	+18.6 (B) +70.8 (N)	+36.2
$(CH_3)_2C + B_8N_8H_{10}$	+1.95	−0.480 (B) +25.7 (N)	−23.3
$(CH_3)_2Si + B_8N_8H_{10}$	+21.6	+8.51 (B) +46.0 (N)	+15.2
$(CH_3)_2Ge + B_8N_8H_{10}$	+27.6	+13.3 (B) +58.0 (N)	+32.6
$(CH_3)_2Sn + B_8N_8H_{10}$	+29.4	+20.1 (B) +66.7 (N)	+50.0
$(CH_3)_2Pb + B_8N_8H_{10}$	+37.0	+26.9 (B) +84.1 (N)	+72.4

[a] All data were obtained by the B3LYP/LANL2DZ approach for eqs 2 and 4, respectively. The energy is given with respect to the reactants in the respective reaction. Potential energy surfaces for the addition of XH_2 to the SWBNNT are summarized in Figure 6. [b] Singlet and triplet energy splitting for the Me_2X species. A positive value means the singlet is the ground state. [c] B and N stand for the B attack (**1a**) and N attack (**1b**), respectively.

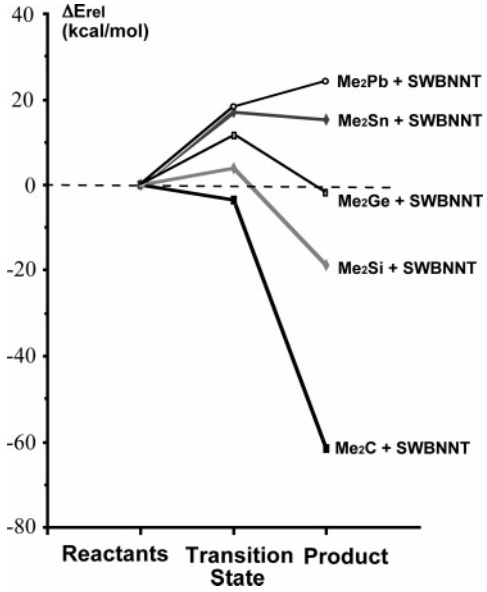

Figure 6. Potential energy surfaces for the cycloadditions of various $(CH_3)_2X$ to SWBNNT (only B attack). The relative energies are taken from the B3LYP/LANL2DZ level as given in Table 6. For B3LYP optimized structures of the stationary points, see Table 4 and Supporting Information.

these transition states is the three-center pattern involving the group 14 element X, boron, and nitrogen. Decomposition of the imaginary mode into internal coordinate displacements shows the major component to be both X−B and X−N bond forming, as one would expect for a true addition TS. Apparently, the transition states connect the corresponding reactants to the addition products.

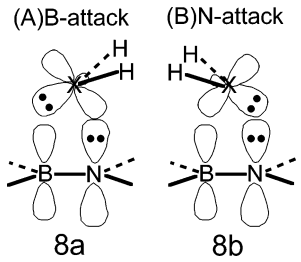

Second, as can be seen from Table 6, the activation barriers with respect to the corresponding reactants for both B-attack and N-attack reaction paths increase in the order (in kcal/mol) Me_2C (−3.4) < Me_2Si (+4.0) < Me_2Ge (+12) < Me_2Sn (+16) < Me_2Pb (+19) and Me_2C (+19) < Me_2Si (+34) < Me_2Ge (+45) < Me_2Sn (+53) < Me_2Pb (+71), respectively. In other words, irrespective of reaction pathway, the greater the atomic number of the X center, the higher the cycloaddition barrier. On this basis, one may therefore conclude that the carbenic addition reactivity decreases in the order C > Si ≫ Ge > Sn > Pb. Moreover, the model calculations also suggest that the cycloaddition of Me_2X to the SWBNNT via path A is essentially kinetically more favorable than that via path B.

It is noted that the polarization of the boron−nitrogen moiety occurs in the sense B^+-N^-, as expected from the eletronegativity difference between boron and nitrogen atoms. Hence, this polarity leads to a larger coefficient at the nitrogen atom, whereas a smaller coefficient at the boron atom. See **8a** (B attack) and **8b** (N attack). This, in turn, makes the nucleophilic attack of the lone-pair orbital of Me_2X become more favorable toward the boron atom, while the empty p orbital of Me_2X can serve as an electronic acceptor for electronic charge from the p−π orbital of nitrogen as shown in **8a**. Accordingly, our theoretical findings show that in the addition of the Me_2X species, it is easier for them to add to the sidewall of the SWBNNT via the B-attack pathway.[29]

Third, like the SWBNNT cycloaddition eq 2, there are also two paths for the reaction of $(CH_3)_2X$ with $B_8N_8H_{10}$, eq 4. Basically, the results for the addition of $(CH_3)_2X$ to $B_8N_8H_{10}$ (**7**) are, at least qualitatively, consistent with the order of addition reactivity discussed above: C > Si > Ge > Sn > Pb, as shown in Table 6. Moreover, the B3LYP calculations also indicate that, for $B_8N_8H_{10}$ cycloadditions, path A (B attack, see **8a**) is kinetically much more favorable than path B (N attack, see **8b**) for a given central atom X. Again, the reason for this is because the electronic repulsion between $(CH_3)_2X$ and the N atom in the B═N bond of $B_8N_8H_{10}$ is much larger than that between $(CH_3)_2X$ and the B atom.

Fourth, as expected for a [1 + 2] cycloaddition, the $(CH_3)_2X$ molecule is coordinated to the B═N fragment in an η^3 fashion via two X−B and X−N σ bonds, with the C−X−C plane nearly parallel to the B═N coordination plane of SWBNNT. Similar to the case of $(CH_3)_2X$ + SWCNT, our computational results indicate that the coordinated B−N bonds in the cycloadducts are completely broken. Namely, all the (5,5) SWBNNT adducts studied in this work prefer opened over closed three-membered ring structures. For example, as shown in Table 4, the B3LYP/LANL2DZ calculations estimate the coordinated B−N bond lengths to be 2.24 Å (Me_2C-SWBNNT-Pro), 2.49 Å (Me_2Si-SWBNNT-Pro), 2.51 Å (Me_2Ge-SWBNNT-Pro), 2.53 Å (Me_2Sn-SWBNNT-Pro), and 2.55 Å (Me_2Si-SWBNNT-Pro), which are all much larger than that of pristine SWBNNT (1.46 Å). The same phenomena can also be found in the smaller model system of $(CH_3)_2X$ (**1**−**5**) + $B_8N_8H_{10}$ (**7**). As seen in Table 5, the B3LYP results predict the coordinated B−N bond distances of 2.20, 2.44, 2.39, 2.46, and 2.52 Å for Me_2C-$B_8N_8H_{10}$-Pro, Me_2Si-$B_8N_8H_{10}$-Pro, Me_2Ge-$B_8N_8H_{10}$-Pro, Me_2Sn-$B_8N_8H_{10}$-Pro, and Me_2Sn-$B_8N_8H_{10}$-Pro, respectively, much larger than that calculated for prime $B_8N_8H_{10}$ (1.46 Å). As there are no relevant experimental and theoretical data on such systems, the above result is a prediction.

Fifth, from the above analysis, it is easy to see that the theoretical trend for carbenic activity toward the sidewall of a SWBNNT is in general agreement with that toward the B═N double bond of $B_8N_8H_{10}$ (**7**). Nevertheless, cycloaddition to a SWBNNT, eq 2, is calculated to have a smaller barrier height and to be more exothermic (or less endothermic) than to $B_8N_8H_{10}$, eq 4, for the same $(CH_3)_2X$ reactant. This is probably related to the fact that electronic repulsion between $(CH_3)_2X$ and the sidewall of a SWBNNT is greater than that between $(CH_3)_2X$ and *planar* $B_8N_8H_{10}$.

In summary of this section, the B-attack path is kinetically much more favorable than the N-attack path. Nevertheless, regardless of which reaction pathway is considered, the carbenic addition reactivity to SWBNNT sidewalls decreases in the order C > Si ≫ Ge > Sn > Pb. That is to say, the more electronegative the central atom X of $(CH_3)_2X$, the lower the activation barrier and the more exothermic is its cycloaddition to a SWBNNT. Moreover, the cycloaddition of the $(CH_3)_2X$ species to SWBNNTs becomes more endothermic (or less exothermic) down the column of group 14 elements, reflecting the weaker X−B and X−N bonds as X changes from C to Pb. Further, our theoretical investigations suggest that the sidewall of SWBNNTs should be opened by chemical modifications. Besides these, since the potential energy profiles of the SWBNNT and $B_8N_8H_{10}$ cycloaddition reactions are qualitatively similar, knowledge of

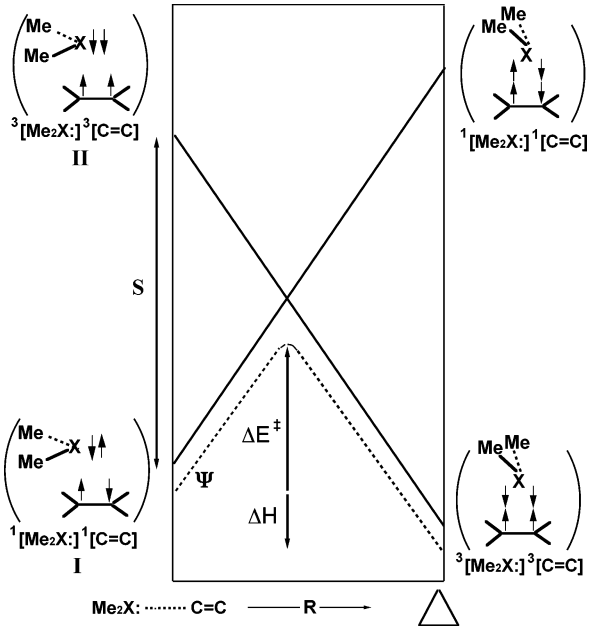

Figure 7. Energy diagram for an addition reaction showing the formation of a potential energy curve (Ψ) by mixing two configurations: the reactant configuration and the product configuration. In the reactants, they are separated by an energy gap *S*. Configuration mixing near the crossing point causes an avoided crossing (dotted line). See the text.

the latter can be used to provide qualitatively correct information about the former.

IV. The Configuration Mixing Model

According to our theoretical analysis, all our computational results can be rationalized on the basis of a configuration mixing (CM) model which was developed by Pross and Shaik.[37] In this section we show how concepts deduced from the CM model can be used to predict the relative reactivity of the reactants.

Although in principle many electron configurations of the species involved in the addition reaction contribute to the precise form of the energy surface,[37] there are only two predominant configurations that contribute significantly to the total wave function Ψ and, in turn, to the potential energy surface, See Figure 7. One is the reactant ground-state configuration that ends up as an excited configuration in the product region. The other is the excited configuration of the reactants that correlates with the ground state of the products.

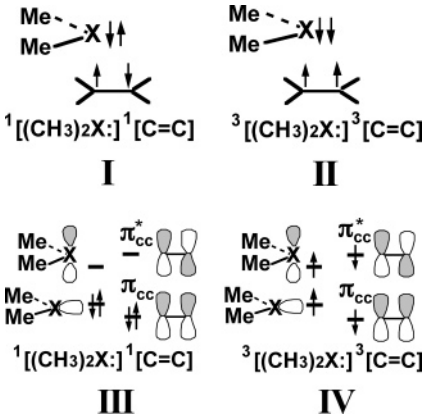

The key valence bond (VB) configurations for the cycloaddition reaction are illustrated in **I** and **II**, while the key molecular orbital (MO) configurations are illustrated in **III** and **IV**.[37] The VB configuration **I**, labeled $^1[(CH_3)_2X:]^1[C{=}C]$, is termed the *reactant configuration* because this configuration is a good descriptor of the reactants; the two electrons on the $(CH_3)_2X$ moiety are spin-paired to form the lone pair, while the two π electrons on the [C=C] species form a π bond. On the other hand, configuration **II** is the VB *product configuration*. It might initially appear strange that triplet pairs are incorporated into the description of a singlet $(CH_3)_2X$ addition reaction. In reality, however, there is no actual spin change here because, despite the fact that $^3[(CH_3)_2X:]^3[C{=}C]$ appears to contain two triplet pairs, the overall spin state of $^3[(CH_3)_2X:]^3[C_2H_4]$ remains a singlet. Moreover, it is a doubly excited configuration only in the reactant geometry. In terms of the product geometry, it is not an excited configuration at all, just the configuration that describes the ground-state addition products.[37] The MO representations of VB configurations **I** and **II** are shown in **III** and **IV**, respectively. A schematic energy plot of **I** and **II** (or **III** and **IV**) for a cycloaddition reaction as a function of the reaction coordinate (the approach of a $(CH_3)_2X$ to the [C=C] molecule), is illustrated in Figure 7. The ground-state reaction profile, obtained by the mixing of reactant and product configurations, is indicated by the dashed curve, and exhibits an activation energy barrier. Thus, it is the avoided crossing of these two configurations that leads to the simplest description of the ground-state energy profiles for addition reactions of the $(CH_3)_2X$ species to the SWCNT and SWBNNT.[37]

In the basis of Figure 7 for barrier formation in SWCNT and SWBNNT cycloaddition reactions, we are now in a position to provide an insight into the parameters that are likely to affect reactivity in these systems. The energy of point **II** (left in Figure 7), the anchor point for $^3[(CH_3)_2X:]^3[C{=}C]$ in the reactant geometry, will be governed by the singlet−triplet energy gap for both $(CH_3)_2X$ and SWCNT (or SWBNNT). i.e., ΔE_{st} ($=E_{triplet} - E_{singlet}$ for $(CH_3)_2X:$) + $\Delta E_{\pi\pi}^*$ ($=E_{triplet} - E_{singlet}$ for SWCNT or SWBNNT). It must be emphasized that the barrier of the chemical reaction is caused by the promotion energy (*S*) that is nonzero as shown in Figure 7. The decrease of *S* ($S = \Delta E_{st} + \Delta E_{\pi\pi}^*$) also stabilizes the product and makes reaction enthalpy ΔH more exothermic.[38] In other words, the smaller the promotion energy *S*, the smaller the $\Delta E_{st} + \Delta E_{\pi\pi}^*$ value, the lower the activation barrier, and the larger the exothermicity.[37] Bearing the above analysis in mind, we shall explain the origin of the observed trends as shown previously in the following discussion:

Why does the ease of the cycloaddition of $(CH_3)_2X$ to the SWCNT and SWBNNT decrease in the order C > Si > Ge > Sn > Pb?

The driving force of this can be traced back to the singlet−triplet energy gap (ΔE_{st}) of a six valence electron $(CH_3)_2X$. It is well established that the electronegativity of the central X atom is greater, the smaller the singlet−triplet splitting of an $(CH_3)_2X$ species.[39] In contrast to the carbenes, all silylenes, germylenes, stannylenes, and plumbylenes characterized to date have exclusively singlet ground states, with the energy of the singlet−triplet energy separation increasing with increasing atomic mass of the group-14 element,[40] which has been confirmed by our B3LYP/LANL2DZ calculations as given in Tables 3 and 6. As analyzed above, if $\Delta E_{\pi\pi}^*$ is a constant, the smaller the ΔE_{st} of $(CH_3)_2X$, the lower the barrier height and the larger the exothermicity, and, in turn, the faster the three-membered ring formation reaction. Indeed, our theoretical calculations confirm this prediction and suggest an increasing trend in ΔE_{st} for $(CH_3)_2C$ (+2.0 kcal/mol)[41] < $(CH_3)_2Si$ (+22 kcal/mol)[42] < $(CH_3)_2Ge$ (+28 kcal/mol) < $(CH_3)_2Sn$ (+29 kcal/

mol) < $(CH_3)_2Pb$ (+37 kcal/mol). From Table 3, it is readily seen that this result is in full accord with the trend in activation energy and reaction enthalpy ($\Delta E^{\ddagger}$, ΔH) for SWCNT cycloadditions which are $(CH_3)_2C$ (+3.2, −60) < $(CH_3)_2Si$ (+6.1, −19) < $(CH_3)_2Ge$ (+14, +0.58) < $(CH_3)_2Sn$ (+24, +21) < $(CH_3)_2Pb$ (+49, +50) kcal/mol. Likewise, the same trend can be found in the SWBNNT cycloadditions as follows (for the B-attack path): $(CH_3)_2C$ (−3.4, −62) < $(CH_3)_2Si$ (+4.0, −19) < $(CH_3)_2Ge$ (+12, −1.8) < $(CH_3)_2Sn$ (+17, +15) < $(CH_3)_2Pb$ (+19, +36) kcal/mol, respectively. Moreover, the same phenomenon can also be seen in both $C_{16}H_{10}$ (**6**) and $B_8N_8H_{10}$ (**7**) systems, which will not be discussed further here.

V. Conclusion

This study has provided the first theoretical demonstration concerning the reaction trajectory and theoretical estimation of the activation energy and reaction enthalpy for the processes in which a methyl-substituted carbene species, $(CH_3)_2X$, adds to a SWCNT or SWBNNT sidewall. Indeed, Understanding the chemistry of C and BN nanotubes is a crucial step toward their ultimate practical use. Our theoretical investigations suggest that the bonding nature at the reacting group 14 element center (X) should play a decisive role in such cycloaddition reactions, since it is shown that an electronegative center X can result in a lower activation energy as well as a higher exothermicity for its addition to the SWCNT and SWBNNT. In addition, the DFT results demonstrate that such cycloaddition reactions involve a three-membered ring transition state and proceed in a concerted manner without further reaction intermediates. Moreover, our theoretical observations indicate that the (5,5) armchair SWCNT and SWBNNT derivatives investigated here have opened structures instead of closed three-membered rings. This means that the sidewall of both (5,5) armchair SWCNTs and SWBNNTs can be readily opened by chemical modifications. Furthermore, from both a kinetic and a thermodynamic viewpoint, the order of reactivity of carbene addition is predicted to be $(CH_3)_2C$ > $(CH_3)_2Si \gg (CH_3)_2Ge$ > $(CH_3)_2Sn$ > $(CH_3)_2Pb$, regardless of whether addition is to a SWCNT or a SWBNNT sidewall. More specifically, $(CH_3)_2C$ and $(CH_3)_2Si$ can readily add to the sidewalls of SWCNT and SWBNNT, whereas $(CH_3)_2Ge$, $(CH_3)_2Sn$, and $(CH_3)_2Pb$ are unreactive toward them.[43]

Besides this, the model calculations indicate that the singlet−triplet splitting of a carbene species ($(CH_3)_2X$) can be used as a diagnostic tool to predict the reactivities of various carbene analogues. From this finding, one may thus design carbene analogues which can effectively functionalize the sidewalls of both C and BN nanotubes. As a result, supposing the central atom X is a constant, substitution effects should also play a prominent role in the chemical functionalization of both C and BN nanotubes. For instance, it is well-known that electron-donating or bulky substituents on the carbene species will result in a smaller ΔE_{st}[33] and, in turn, will facilitate the chemical functionalization of both C and BN nanotubes. On the other hand, the present theoretical results demonstrate that the sidewall reactivity of C and BN nanoubes closely resembles that of their smaller fragments (such as $C_{16}H_{10}$, **6**, and $B_8N_8H_{10}$, **7**, respectively). Accordingly, the use of the latter smaller models, from which one may easily obtain a singlet−triplet energy gap, can allow one to assess quickly the relative sidewall reactivities of various nanotubes without specific knowledge of the actual energies of the interactions involved. Despite its simplicity, our approach can provide experimentalists with important insights into the factors controlling the activation energies for functionalization of nanotube sidewalls and thus permit them to predict the reactivity of some known and unknown nanotubes. The predictions may be useful as a guide to future synthetic efforts and to indicate problems that merit further study by both theory and experiment.

It is hoped that our study will stimulate further research into the subject.

Acknowledgment. The author is grateful to the National Center for High-Performance Computing of Taiwan for generous amounts of computing time. He also thanks the National Science Council of Taiwan for the financial support. In particular, he wishes to thank Professor Feng-Yin Li (National Chung Hsing University) and Dr. Li Ta-Wei (National Chiao Tung University) for encouragement and much skillful assistance. Special thanks are also due to one anonymous referee for very helpful suggestions and comments.

Supporting Information Available: A listing of Cartesian coordinates calculated for stationary points at the B2LYP level. This material is available free of charge via the Internet at http://pubs.acs.org.

References and Notes

(1) Iijima, S. *Nature* **1991**, *354*, 56.

(2) For reviews and pertinent references see: (a) Ajayan, P. M. *Chem. Rev.* **1999**, *99*, 1787. (b) Rao, N. R.; Govindaraj, A. *Acc. Chem. Res.* **2002**, *35*, 998. (c) Andrews, R.; Jacques, D.; Qian, D.; Rantell, T. *Acc. Chem. Res.* **2002**, *35*, 1008. (d) Ouyang, M.; Huang, J.-L.; Lieber, C. M. *Acc. Chem. Res.* **2002**, *35*, 1018. (e) Avouris, P. *Acc. Chem. Res.* **2002**, *35*, 1026. (f) Dai, H. *Acc. Chem. Res.* **2002**, *35*, 1035. (g) Zhou, O.; Shimoda, H.; Gao, B.; Oh, S.; Fleming, L.; Yue, G. *Acc. Chem. Res.* **2002**, *35*, 1045. (h) Sloan, J.; Kirkland, A. I.; Hutchison, J. L.; Green, M. L. H. *Acc. Chem. Res.* **2002**, *35*, 1054. (i) Charlier, J.-C. *Acc. Chem. Res.* **2002**, *35*, 1063. (j) Dresselhaus, M. S.; Dresselhaus, G.; Jorio, A.; Souza Filho, A. G.; Pimenta, M. A.; Satio, R. *Acc. Chem. Res.* **2002**, *35*, 1070. (k) Fischer, J. E. *Acc. Chem. Res.* **2002**, *35*, 1079. (l) Khabashesku, V. N.; Billups, W. E.; Margrave, J. L. *Acc. Chem. Res.* **2002**, *35*, 1087. (m) Bahr, J. L.; Tour, J. M. *J. Mater. Chem.* **2002**, *12*, 1952. (n) Davis, J. J.; Coleman, K. S.; Azamian, B. R.; Bagshhaw, C. B.; Green, M. L. H. *Chem. Eur. J.* **2003**, *9*, 3721. (o) Joselevich, E. *Angew. Chem., Int. Ed.* **2004**, *43*, 2992.

(3) For reviews and pertinent references see: (a) Sun, Y.-P.; Fu, K.; Lin, Y.; Huang, W. *Acc. Chem. Res.* **2002**, *35*, 1096. (b) Niyogi, S.; Hamon, M. A.; Hu, H.; Zhao, B.; Bhowmik, P.; Sen, R.; Itkis, M. E.; Haddon, R. C. *Acc. Chem. Res.* **2002**, *35*, 1105. (c) Hirsch, A. *Angew. Chem., Int. Ed.* **2002**, *41*, 1853. (d) Tasis, D.; Tagmatarchis, N.; Georgakilas, V.; Prato, M. *Chem. Eur. J.* **2003**, *9*, 4000. (e) Banerjee, S.; Kahn, M. G. C.; Wong, S. S. *Chem. Eur. J.* **2003**, *9*, 1899. (f) Yao, Z.; Braidy, N.; Botton, G. A.; Adronov, A. *J. Am. Chem. Soc.* **2003**, *125*, 16015.

(4) Chen, J.; Hamon, M. A.; Hu, H.; Chen, Y.; Rao, A. M.; Eklund, P. C.; Haddon, R. C. *Science* **1998**, *282*, 95. (b) Bahr, J. L.; Mickelson, E. T.; Bronikowski, M. J.; Smalley, R. E.; Tour, J. M. *Chem. Commun.* **2001**, 193.

(5) Collins, P.; Bradley, K.; Ishigami, M.; Zettl, A. *Science* **2000**, *287*, 1801. (b) Kong, J.; Franklin, N.; Zhou, C.; Chapline, M.; Peng, S.; Cho, K.; Dai, H. *Science* **2000**, *287*, 622. (c) Kong, J.; Chapline, M.; Dai, H. *Adv. Mater.* **2001**, *13*, 1384.

(6) For instance, see: (a) Lago, R. M.; Tsang, S. C.; Lu, K. L.; Chen, Y. K.; Green, M. L. H. *J. Chem, Soc., Chem. Commun.* **1995**, 1355. (b) Ebbesen, T. W. *J. Phys. Chem. Solids* **1996**, *57*, 951. (c) Satishkumar, B. C.; Govindaraj, A.; Mofokeng, J.; Subbanna, G. N.; Rao, C. N. R. *J. Phys. B: At., Mol. Opt. Phys.* **1996**, *29*, 4925. (d) Liu, J.; Rinzler, A. G.; Dai, H. J.; Hafner, J. H.; Bradley, R. K.; Boul, P. J.; Lu, A.; Iverson, T.; Shelimov, K.; Huffman, C. B.; Rodriguez-Macias, F.; Shon, Y. S.; Lee, T. R.; Colbert, D. T.; Smalley, R. E. *Science* **1998**, *280*, 1253. (e) Wong, S. S.; Joselevich, E.; Woolley, A. T.; Cheung, C. L.; Lieber, C. M. *Nature* **1998**, *394*, 52. (f) Hamon, M. A.; Chen, J.; Hu, H.; Chen, Y.; Itkis, M. E.; Rao, A. M.; Eklund, P. C.; Haddon, R. C. *Adv. Mater.* **1999**, *11*, 834. (g) Bettinger, H. F.; Kudin, K. N.; Scuseria, G. E. *J. Am. Chem. Soc.* **2001**, *123*, 12849. (h) Bahr, J. L.; Tour, J. M. *J. Mater. Chem.* **2002**, *12*, 1952. (i) Pantarotto, D.; Partidos, C. D.; Graff, R.; Hoebeke, J.; Briand, J.-P.; Prato, M.; Bianco, A. *J. Am. Chem. Soc.* **2003**, *125*, 6160 and references therein.

(7) Holzinger, M.; Vostrowsky, O.; Hirsch, A.; Hennrich, F.; Kappes, M.; Weiss, R.; Jellen, F. *Angew. Chem., Int. Ed.* **2001**, *40*, 4002. (b) Reference 3c. (c) Holzinger, M.; Abraham, J.; Whelan, P.; Graupner, R.; Ley, L.; Hennrich, F.; Kappes, M.; Hirsch, A. *J. Am. Chem. Soc.* **2003**, *125*, 8566.

(8) For reviews and pertinent references see: Rao, C. N. R.; Nath, M. *J. Chem. Soc., Dalton Trans.* **2003**, 1.

(9) Blasé, X.; Rubio, A.; Louie, S. G.; Cohen, M. L. *Europhys. Lett.* **1994**, *28*, 335. (b) Rubio, A.; Corkill, J. L.; Cohen, M. L. *Phys. Rev. B* **1994**, *49*, 5081. (c) Blase, X.; Vita, A. D.; Charlier, J.-C.; Car, R. *Phys. Rev. Lett.* **1998**, *80*, 1666. (d) Hernandez, E.; Goze, C.; Bernier, P.; Rubio, A. *Phys. Rev. Lett.* **1998**, *80*, 4502. (e) Gleize, P.; Schouler, M. C.; Gadelle, P.; Caillet, M. *J. Mater. Sci.* **1994**, *29*, 1575. (f) Gleize, P.; Herreyre, S.; Gadelle, P.; Mermoux, M.; Cheynet, M. C.; Abello, L. *J. Mater. Sci. Lett.* **1994**, *13*, 1413. (g) Chopra, N. G.; Luyken, R. J.; Cherry, K.; Crespi, V. H.; Cohen, M. L.; Louie, S. G.; Zettl, A. *Science* **1995**, *269*, 966. (h) Loiseau, A.; Willaime, F.; Demoncy, N.; Hug, G.; Pascard, H. *Phys. Rev. Lett.* **1996**, *76*, 4737. (I) Menon, M.; Srivastava, D. *Chem. Phys. Lett.* **1999**, *307*, 407.

(10) Tenne, R.; Margulis, L.; Genut, M.; Hodes, G. *Nature* **1992**, *360*, 444. (b) Hamilton, E. J. M.; Dolan, S. E.; Mann, C. M.; Colijn, H. O.; McDonald, C. A.; Shore, S. G. *Science* **1993**, *260*, 659. (c) Stephan, O.; Ajayan, P. M.; Colliex, C.; Redlich, P.; Lambert, J. M.; Bernier, P.; Lefin, P. *Science* **1994**, *266*, 1683. (d) Weng-Sieh, Z.; Cherrey, K.; Chopra, N. G.; Blasé, X.; Miyamato, Y.; Rubio, A.; Cohen, M. L.; Louie, S. G.; Zettl, A.; Gronsky, R. *Phys. Rev. B* **1995**, *51*, 11229. (e) Chopra, N. G.; Luken, R. J.; Cherrey, K.; Crespi. V. H.; Cohen, M. L.; Louie, S. G.; Louie, A.; Zettl, A. *Science* **1995**, *269*, 966. (f) Golberg, D.; Bando, Y.; Eremets, M.; Takemura, K.; Kurashima, K.; Yusa, H. *Appl. Phys. Lett.* **1996**, *69*, 2045. (g) Loiseau, A.; Willaime, F.; Demoncy, N.; Hug, G.; Pascard, H. *Phys. Rev. Lett.* **1996**, *76*, 4737. (h) Yu, D. P.; Sun, X. S.; Lee, C. S.; Bello, I.; Lee, S. T., Gu, H. D.; Leung, K. M.; Zhou, G. W.; Dong, Z. F.; Zhang, Z. *Appl. Phys. Lett*. **1998**, *72*, 1966. (i) Zhou, G. W.; Zhang, Z.; Bai, Z. G.; Yu, D. P. *Solid State Commun.* **1999**, *109*, 555. (j) Chen, Y.; Gerald, J. F.; Williams, J. S.; Bulcock, S. *Chem. Phys. Lett.* **1999**, *299*, 260. (k) Saito, Y.; Maida, M. *J. Phys. Chem. A* **1999**, *103*, 1291. (l) Pokropivny, V. V.; Shorokod, V. V.; Oleinik, G. S.; Kurdyumov, A. V.; Bartnitskaya, T. S.; Pokropivny, A. V.; Sisonyuk, A. G.; Sheichenko, D. M. *J. Solid State Chem.* **2000**, *154*, 214. (m) Ma, R.; Bando, Y.; Sato, T. *Chem. Phys. Lett.* **2001**, *337*, 61. (n) Deepak, F. L.; Vinod, C. P.; Mukhopadhyay, K.; Govindaraj, A.; Rao, C. N. R. *Chem. Phys. Lett.* **2002**, *353*, 345. (o) Lourie, O. R.; Jones, C. R.; Bertlett, B. M.; Gibbons, P. C.; Ruoff, R. S.; Buhro, W. E. *Chem. Mater.* **2002**, *12*, 1808.

(11) Golberg, D.; Bando, Y.; Kurashima, K.; Sato, T. *Scr. Mater*. **2001**, *44*, 1561.

(12) Meunier, V.; Roland, C.; Bernholc, J.; Nardelli, M. B. *Appl. Phys. Lett.* **2002**, *81*, 46. (b) Golberg, D.; Bando, Y.; Fushimi, K.; Mitome, M.; Bourgeois, L.; Tang, C.-C. *J. Phys. Chem. B* **2003**, *107*, 8726.

(13) While our study was in progress, Han and Zettle reported a novel experimental result concerning functionalized BN nanotubes with a SnO_2 coating. See: Han, W.; Zettl, A. *J. Am. Chem. Soc.* **2003**, *125*, 2062.

(14) Guo, T.; Nikolaev, P.; thess, A.; Colbert, D. T.; Smalley, R. E. *Chem. Phys. Lett.* **1995**, *243*, 329. (b) Terrones, M.; Hsu, W. K.; Terrones, H.; Zhang, J. P.; Ramos, S.; Hare, J. P.; Castillo, R.; Prassides, K.; Cheetham, A. K.; Kroto, H. W.; Walton, D. R, M. *Chem. Phys. Lett.* **1996**, *259*, 1996. (c) Redlich, P. H.; Loeffler, J.; Ajayan, P. M.; Bill, J.; Aldinger, F.; Ruhle, M. *Chem. Phys. Lett.* **1996**, *260*, 465. (d) Golberg, D.; Bando, Y.; Eremets, M.; Takemura, K.; Kurashima, K.; Tamiya, K.; Yusa, H. J. *Chem. Phys, Lett*. **1997**, *279*, 191. (e) Golberg, D.; Bando, Y.; Eremets, M.; Kurashima, K.; Tamiya, K.; Takemura, K.; Yusa, H. J. *Chem. Phys. Lett*. **1997**, *46*, 281. (f) Cumings, J.; Zettl, A. *Chem. Phys. Lett*. **2000**, *316*, 211.

(15) Bauschlicher, C. W., Jr. *Chem. Phys. Lett*. **2000**, *322*, 237. (b) Froudakis, G. E. *Nano Lett.* **2001**, *1*, 179. (c) Bauschlicher, C. W., Jr. *Nano Lett.* **2001**, *1*, 223. (d) Basiuk, V. A.; Basiuk, E. V.; Saniger-Blesa, J.-M. *Nano Lett.* **2001**, *1*, 657. (e) Banerjee, S.; Hemraj-Benny, T.; Balasubramanian, M.; Fischer, D. A.; Misewich, J. A.; Wong, S. S. *Chem. Commun*. **2004**, 772. (f) Joselevich, E. *ChemPhysChem*. **2004**, *5*, 619. (g) Bianco, A.; Kostarelos, K.; Partidos, C. D.; Prato, M. *Chem. Commun*. **2005**, 559.

(16) Becke, A. D. *Phys. Rev. A* **1988**, *38*, 3098. (b) Becke, A. D. *J. Chem. Phys.* **1993**, *98*, 1372. (c) *J. Chem. Phys.* **1993**, *98*, 5648.

(17) Lee, C.; Yang, W.; Parr, R. G. *Phys. Rev. B* **1988**, *37*, 785.

(18) The synthesis of single-walled nanotubes has been described previously, see: (a) Guo, T.; Nikolaev, P.; Thess, A.; Colbert, D. T.; Smalley, R. E. *Chem. Phys. Lett.* **1995**, *243*, 49. (b) Rinzler, A. G.; Liu, J.; Dai, H.; Nikolaev, P.; Huffman, C.; Rodriquez-Macias, F. J.; Boul, P. J.; Lu, A. H.; Heymann, D. J.; Collbert, D. T.; Lee, R. S.; Fischer, J. E.; Rao, A. M.; Eklund, P. C.; Smalley, R. E. *Appl. Phys. Lett*. **1998**, *67*, 29. (d) Although single isolated carbon nanotubes have been reported (see: Bethune, D. S.; Kiamg, C. H.; de Vries, M. S.; Gorman, G.; Savoy, R.; Vasquez, J.; Beyers, R. *Nature* **1993**, *363*, 605), the single-walled nanotubes just like the multiwalled nanotubes tend to form bundles of nearly parallel tubes. See: Iijima, S.; Ichihashi, T. *Nature* **1993**, *63*, 603.

(19) Okotrub, A. V.; Bulusheva, L. G.; Tomanek, D. *Chem. Phys. Lett*. **1998**, *289*, 341.

(20) Srivastava, D.; Brenner, D. W.; Schall, J. D.; Ausman, K. D.; Yu, M.; Ruoff, R. S. *J. Phys. Chem. B* **1999**, *103*, 4330. (b) Kelly, K. F.; Chiang, I. W.; Mickelson, E. T.; Hauge, R. H.; Margrave, J. L.; Wang, X.; Scuseria, G. E.; Radloff, C.; Halas, N. J. *Chem. Phys. Lett.* **1999**, *313*, 445.

(21) Chen, J.; Haddon, R. C.; Fang, S.; Rao, A. M.; Lee, W. H.; Dickey, E. C.; Grulke, E. A.; Pendergrass, J. C.; Chavan, A.; Haley, B. E.; Smalley, R. E. *J. Mater. Res.* **1998**, *13*, 2423. (b) Mickelson, E. T.; Huffman, C. B.; Rinzler, A. G.; Smalley, R. E.; Hauge, R. H.; Margrave, J. L. *Chem. Phys. Lett.* **1998**, *296*, 188.

(22) Bulusheva, L. G.; Okotrub, A. V.; Romanov, D. A.; Tomanek, D. *J. Phys. Chem.* **1998**, *102*, 975. (b) Kelly, K. F.; Chiang, I. W.; Mickelson, E. T.; Hauge, R. H.; Margrave, J. L.; Wang, X.; Scuseria, G. E.; Radloff, C.; Halas, N. J. *Chem. Phys. Lett.* **1999**, *313*, 445. (c) Liang, W. Z.; Wang, X. J.; Yokojima, S.; Chen, G. H. *J. Am. Chem. Soc.* **2000**, *122*, 11129. (d) Turker, L.; Bayer, I. *J. Phys. Chem. Solids* **2000**, *61*, 1041. (e) Mann, D. J.; Halls, M. D.; Hase, W. L. *J. Phys. Chem.* **2002**, *106*, 12418. (f) Clare, B. W.; Kepert, D. L. *Inorg. Chim. Acta* **2003**, *343*, 1.

(23) Rochefort, A.; Salahub, D. R.; Avouris, P. *J. Phys. Chem. B* **1999**, *103*, 641. (b) Lier, G. V.; Alsenoy, C. V.; Doren, V. V.; Geerlings, P. *Chem. Phys. Lett*. **2000**, *326*, 181. (c) Kar, T.; Pattanayak, J.; Scheiner, S. *J. Phys. Chem. A* **2001**, *105*, 10397.

(24) Maseras, F.; Morokuma, K. *J. Comput. Chem.* **1995**, *16*, 1770. (b) Humbel, S.; Sieber, S.; Morokuma, K. *J. Chem. Phys.* **1996**, *105*, 1959. (c) Svensson, M.; Humbel, S.; Froese, R. D.; Matsubara, T.; Sieber, S.; Morokuma, K. *J. Phys. Chem.* **1996**, *100*, 19357. (d) Dapprich, S.; Komaromi, I.; Byun, K. S.; Morokuma, K.; Frisch, M. J. *J. Mol. Struct.* (*Theochem*) **1999**, *461/462*, 1.

(25) Bauschlicher, C. W., Jr.; So, C. R. *Nano Lett.* **2002**, *2*, 337. (b) Lu, X.; Tian, F.; Zhang, Q. *J. Phys. Chem. B* **2003**, *107*, 8388. (c) Kar, T.; Akdim, B.; Duan, X.; Pachter, R. *Chem. Phys. Lett.* **2004**, *392*, 176.

(26) Chen, Z.; Nagase, S.; Hirsch, A.; Haddon, R. C.; Thiel, W.; Schleyer, P. von R. *Angew. Chem., Int. Ed.* **2004**, *43*, 1552.

(27) Chu, Y.-Y.; Su, M.-D. *Chem. Phys. Lett*. **2004**, *394*, 231. (b) Bettinger, H. F. *Org. Lett.* **2004**, *6*, 731.

(28) The (5,5) armchair SWCNT and SWBNNT derivatives investigated here have opened structures instead of three-membered rings. On the other hand, it is well-known that carbenes add to olefins to give cyclopropanes. The reason for such a difference between them is presumably due to the bond-angle strain, which contributes to their ease of opening. Certainly, to obtain a better understanding of such cheletropic reactions in single-walled nanotube systems requires further computational studies as well as experiments. Such studies, however, are beyond the scope of the present work. Also see ref 29.

(29) For reviews about carbene cycloadditions see: (a) Gilchrist, T. L.; Storr, R. C., *Organic Reactions and Orbital Symmetry*; Cambridge University Press: Landon, 1972; pp 90−140. (b) Isaacs, N. *Physical Organic Chemistry*; Longman Scientific & Technical: London, 1995; pp 599−753. (c) Lowry, T. H.; Richardson, K. S. *Mechanism and Theory in Organic Chemistry*; Harper Collins Publishers: New York, 1987; pp 567−660. (d) Carroll, F. A. *Perspectives on Structure and Mechanism in Organic chemistry*; Brooks/Cole Publishing Co.: New York, 1998; pp 548−640.

(30) Hoffmann, R.; Shaik, S.; Hiberty, P. C. *Acc. Chem. Res.* **2003**, *36*, 750.

(31) Dunning, T. H., Jr.; Hay, P. J. In *Modern Theoretical Chemistry*; Schaefer, H. F., III, Ed.; Plenum: New York, 1976; pp 1−28. (b) Hay, P. J.; Wadt, W. R. *J. Chem. Phys*. **1985**, *82*, 284.

(32) Frisch, M. J.; Trucks, G. W.; Schlegel, H. B.; Scuseria, G. E.; Robb, M. A.; Cheeseman, J. R.; Zakrzewski, V. G.; Montgomery, J. A., Jr.; Stratmann, R. E.; Burant, J. C.; Dapprich, S.; Millam, J. M.; Daniels, A. D.; Kudin, K. N.; Strain, M. C.; Farkas, O.; Tomasi, J.; Barone, V.; Cossi, M.; Cammi, R.; Mennucci, B.; Pomelli, C.; Adamo, C.; Clifford, S.; Ochterski, J.; Petersson, G. A.; Ayala, P. Y.; Cui, Q.; Morokuma, K.; Malick, D. K.; Rabuck, A. D.; Raghavachari, K.; Foresman, J. B.; Cioslowski, J.; Ortiz, J. V.; Baboul, A. G.; Stefanov, B. B.; Liu, Liashenko, G.; Piskorz, A.; Komaromi, P.; I.; Gomperts, R.; Martin, R. L.; Fox, D. J.; Keith, T.; Al-Laham, M. A.; Peng, C. Y.; Nanayakkara, A.; Gonzalez, C.; Challacombe, M.; Gill, P. M. W.; Johnson, B.; Chen, W.; Wong, M. W.; Andres, J. L.; Gonzalez, C.; Head-Gordon, M.; Replogle, E. S. and Pople, J. A. *Gaussian 03*; Gaussian, Inc.: Wallingford, CT, 2004.

(33) The reason for choosing the armchair (5,5) SWCNT and SWBNNT as model reactants in the present study is as follows. According to the work of Chen, Thiel, and Hirsch (Chen, Z.; Thiel, W.; Hirsch, A. *ChemPhysChem* **2003**, *4*, 93.), it was shown that the reactivity of (*n*,*n*) SWCNTs toward sidewall addition depends strongly on the diameter of the tube and more precisely on the pyramidalization angle θ_p of the tube C atom where the addition takes place. Namely, this difference in reactivity increases with increasing pyramidalization angle and decreasing diameter of the tube (ref 6g). As a result, it was decided that the armchair (5,5) nanotube would be a suitable model reactant in the present work.

(34) Nevertheless, from the calculations presented in this work, one may argue that the addition of nucleophilic carbenes generate opened three-membered rings instead of the zwitterionic adducts described in ref 7a. The reason for this is presumably that the carbene species used in Hirsch and co-workers' work is dipyridyl imidazolidene, which contains two nitrogen atoms surrounding the carbene center. That is, the structure of this species is similar to that of 1,3-di(1-adamantyl)imidazol-2-ylidene. In particular, the former has 14 aromatic π electrons, while the latter has only

6 π electrons in the perimeter. This makes the former possess much greater nucleophilicity than the other carbene species studied in this work. As a result, when these carbenes react with carbon nanotubes, the carbene with smaller nucleophilicity would attack a wall C═C p−π bond to generate opened three-membered rings, whereas dipyridyl imidazolidene would attack a wall carbon atom to produce the zwitterionic adducts.

(35) For details concerning the addition of carbene to the ethylene see: Su, M.-D. *J. Phys. Chem.* **1996**, 100, 4339 and references therein. (b) For related references concerning the addition of silylene to the ethylene see: Su, M.-D. *J. Am. Chem. Soc.* **2002**, *124*, 12335. (c) For details concerning the addition of germylene to the ethylene see: Su, M.-D.; Chu, S.-Y. *J. Am. Chem. Soc.* **1999**, *121*, 11478.

(36) Hoffmann, R., *J. Am. Chem. Soc.*, **1968**, *90*, 1475.

(37) Shaik, S.; Schlegel, H. B.; Wolfe, S. *Theoretical Aspects of Physical Organic Chemistry*; Wiley: New York, 1992. (b) Pross, A. *Theoretical and Physical principles of Organic Reactivity*; Wiley: New York, 1995. (c) Shaik, S. *Prog. Phys. Org. Chem*. **1985**, *15*, 197. (d) The first paper that originated the CM model see: Shaik, S. *J. Am. Chem. Soc*. **1981**, *103*, 3692. (e) About the most updated review of the CM model, one can see: Shaik, S.; Shurki, A. *Angew. Chem., Int. Ed. Engl*. **1999**, *38*, 586.

(38) It has to be mentioned that apparent $\Delta E^{\ddagger}$(activation energy)−ΔH(reaction enthalpy) correlation is just secondary and does not establish a cause and effect relationship between the two quantities. For details, see ref 37c.

(39) Carter, E. A.; Goddard, W. A., III *J. Phys. Chem*. **1986**, *90*, 998. (b) *J. Phys. Chem.* **1987**, *91*, 4651. (c) *J. Chem. Phys*. **1988**, *88*, 1752. (d) Shin, S. K.; Goddard, W. A., III; Beauchamp, J. L. *J. Phys. Chem.* **1990**, *94*, 6963. (e) Irikura, K. K.; Goddard, W. A., III; Beauchamp, J. L. *J. Am. Chem. Soc.* **1992**, *114*, 48.

(40) Apeloig, Y. *The Chemistry of Organic Silicon Compounds*, Part I; Patai, S.; Rappoport, Z., Eds.; Wiley: Chichester, 1998; 57 pp.

(41) High level ab initio calculations predict dimethylcarbene to have a singlet ground state with a singlet−triplet splitting of about 1.5 kcal/mol. See: (a) Matzinger, S.; Fulscher, M. P. *J. Phys. Chem.* **1995**, *99*, 10747. (b) Sulzbach, H. M.; Platz, M. S.; Schaefer, H. F., III; Hadad, C. M. *J. Am. Chem. Soc.* **1997**, *119*, 5682 and references therein.

(42) DFT calculations predict dimethylsilylene to have a singlet ground state with a singlet−triplet splitting of about 24−26 kcal/mol. See: Yoshida, M.; Tamaoki, N. *Organometallics* **2002**, *21*, 2587.

(43) Furthermore, these conclusions should be extended to apply to other carbene-like species (such as nitrenes, ref 7). However, this study is beyond the scope of the present work. Future work along this line is in progress and will be published elsewhere.